Systematic method of applying ANN for chemical kinetics reduction in turbulent premixed combustion modeling

ZHOU ZhiJun, LÜ Yu, WANG ZhiHua[*], XU YanWei, ZHOU JunHu & CEN KeFa

State Key Laboratory of Clean Energy Utilization, Department of Energy Engineering, Zhejiang University, Hangzhou 310027, China

A novel method to apply artificial neural network (ANN) for both chemical kinetics reduction and source term evaluation is introduced and tested in direct numerical simulation (DNS) and large eddy simulation (LES) of reactive flows. To gather turbulence affected flame data for ANN training, a new computation-economical method, called 1D pseudo-velocity disturbed flame (PVDF), is developed and used to generate thermo-chemical states independent of the modeled flame. Then a back-propagation ANN is trained using scaled conjugate gradient algorithm to memorize the sample states with reduced orders. The new method is employed in DNS and LES modeling of H_2/air and C_3H_8/air premixed flames experiencing various levels of turbulence. The test result shows that compared to traditional computation with full mechanism and direct integration, this method can obtain quite large speed-ups with adequate prediction accuracy.

ANN, kinetics reduction, LES, DNS

Detailed chemical mechanism has been widely employed to numerically study fundamental phenomena involved in flame turbulence interaction, for example, vortex-induced quenching and re-ignition [1], soot [2] and NO_x [3] formation in turbulent flame and flame propagation [4]. However, huge computational burden is always a knotty event during such researches, which mainly stems from two respects: first, large number of species mass balance equations should be temporally advanced; second, many minor species have much smaller time scales than others so that time-consuming stiff ODE solvers are normally required. As a result, complex calculations involved in chemical source evaluation are continually repeated.

In chemical kinetics reduction field, sensitivity analysis [5], quasi-steady state (QSS) assumption [6] and direct relation graphics (DRG) method [7,8] are often used, while ANN method, a extremely new systemic technique, is seldom seen in previous work. The procedure of using QSS assumption has been shown in Figure 1. However, QSS species concentrations should be first resolved which includes a large amount of algebraic iterations. Therefore, the net efficiency could be undermined [9], and also calculation may be failed if iterations do not converge.

As for the second respect, several approaches to accelerate chemical sources evaluation have already been presented, such as look-up table (LUT) [10] and in situ-adaptive tabulation (ISAT) [11]. However, they are both based on tabulation technique which needs huge memory and a large number of check-up and interpolation operations. Artificial neural network (ANN) method, although it was proposed previously to handle above drawbacks, has got great progress through Sen and Menon's work [12,13]. It has been successfully applied to account for chemical kinetics in LES modeling of turbulent premixed flame with speed-ups even more than 10.

In this paper, we tend to extend the application of ANN method, using it to not only calculate chemical sources but also reduce the detailed mechanism. The initial idea is to construct the direct mapping between non-QSS species concentrations and their reaction rates at plenty of thermal

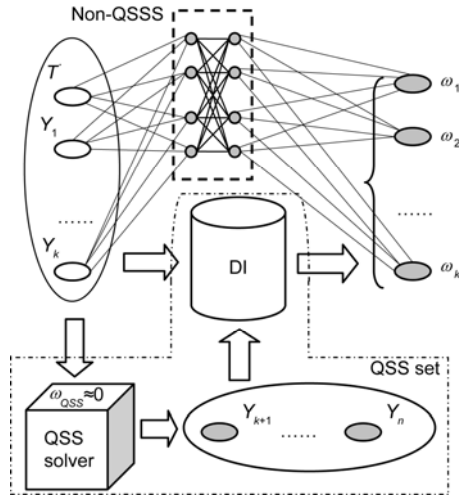*Corresponding author (email: wangzh@zju.edu.cn)

Figure 1 Procedure of using traditional reduced mechanism and ANN-based alternative one (DI means "direct integration").

states considering turbulence effect (see Figure 1). This ANN-based method for chemical kinetics reduction, if demonstrated applicably, can bypass all time-consuming links involved in integration of traditional mechanism and directly offer chemical sources for the mass balance equations of primarily concerned non-QSS species. In other words, it can completely solve the above-mentioned two problems in numerical investigations. Thus, this paper is organized according to the following thread: How is ANN-based method for chemical kinetics reduction constructed? What about the applicability of this method? What is the performance?

1 Construction of ANN-based method for chemical kinetics reduction

This ANN-based method is constructed by gathering thermo-chemical sample states, precluding QSS species and employing ANN to memorize the low-order states. All sample states should be at the specific equivalence ratio Φ with turbulence effect. In [12], sample states were given by DNS of a laminar flame vortex interaction. Although tested performance was satisfactory, this method was very time-consuming. In this paper, an alternative way with largely reduced calculation is presented. To demonstrate the novel method, premixed combustions of H_2/air at Φ=1.0 and C_3H_8/air at Φ=0.65 are modeled using 11-species 21-step [14] and 28-species 73-step [15] mechanisms, respectively. For comparison, no reduction was carried out on H_2/air mechanism, while QSS assumption was imposed on C_3H_8/air combustion process. By adopting the following criterion [6] at laminar C_3H_8/air premixed flame:

$$\frac{\left|\omega_s^P - \omega_s^C\right|}{\max\{\left|\omega_s^P\right|, \left|\omega_s^C\right|\}} \sim 10^{-2}, \tag{1}$$

where ω_s is chemical reaction rate of specie s, superscript P and C represent production and consumption, respectively. 7 QSS species are identified, which are CH, CH_2, C_2H_2, C_2H_3, C_2H_5, C_2H_6 and CH_2CO. This set of QSS species are eliminated from the gathered sample states. Thus, after being trained, the ANN-based method is actually constructed.

1.1 Sample data generation

Sample data for ANN training are initially generated using 1D pseudo-velocity disturbed flame (PVDF) method. The critical idea of this method is to accumulate thermo-chemical state by stepping following equations with original detailed mechanism:

$$\rho \frac{\partial(Y_s)}{\partial t} = -\rho u_t(x)\frac{\partial(Y_s)}{\partial x} - \frac{\partial(\rho Y_s V_s)}{\partial x} - \omega_s, \tag{2}$$

$$c_v\rho\frac{\partial T}{\partial t} = -c_v\rho u_t(x)\frac{\partial(T)}{\partial x} - P\frac{\partial u_t(x)}{\partial x} + \frac{\partial}{\partial x}(\lambda\frac{\partial T}{\partial x})$$
$$+ \sum_s h_s\omega_s - \frac{\partial T}{\partial x}\rho\sum_s Y_s V_s c_{ps}, \tag{3}$$

$$\rho = \frac{P}{R_g T}, \quad V_s = -D_{sm}\frac{W_s}{\overline{W}Y_s}\frac{dX_s}{dx}, \quad \sum Y_s V_s = 0, \tag{4}$$

where ρ is density, Y is the mass fraction , $u_t(x)$ is pseudo-velocity used to get disturbed flame data, V is diffusion velocity, c_v is mixture specific heat capacity at constant volume, T is temperature, P is pressure, λ is thermal conductivity of the mixture, h is standard-state enthalpy, c_p is specific heat capacity at constant pressure, R_g is universal gas constant of the mixture, D_m is mixture-averaged diffusion coefficient, X is volume fraction, W and $\overline{W}$ are molecular weight and mean molecular weight, respectively. Subscript s represent specie s.

1D laminar premixed flame at fixed equivalence ratio (consistent with applied condition) was firstly set to be initial state and then above equations were advanced with 2th-order difference scheme and 1th-order Euler march. To duplicate turbulence effect on flame, $u_t(x)$ is updated at time domain according to an isotropic, homogeneous turbulent kinetic energy spectrum given by [16]

$$E(k) = \frac{32}{3}\sqrt{\frac{2}{\pi}}\frac{u'^2}{k_e}\left(\frac{k}{k_e}\right)^4\exp\left[-2\left(\frac{k}{k_e}\right)^2\right], \tag{5}$$

where k_e is the most energetic wavenumber in adopted energy spectrum, expressed as

$$k_e = \sqrt{\frac{4\varepsilon}{10vu'^2}}, \tag{6}$$

u' is a preset fluctuation velocity controlling turbulence intensity. To let flame experience different level of turbulence, PVDF was run at 7 different u' ranging from 0.5 m/s to u'_{max} for both cases. The basic parameters which characterize the turbulent intensity are given in Table 1. In the following test, u'_{max} is estimated to be 10 m/s for H_2/air case and 5 m/s for
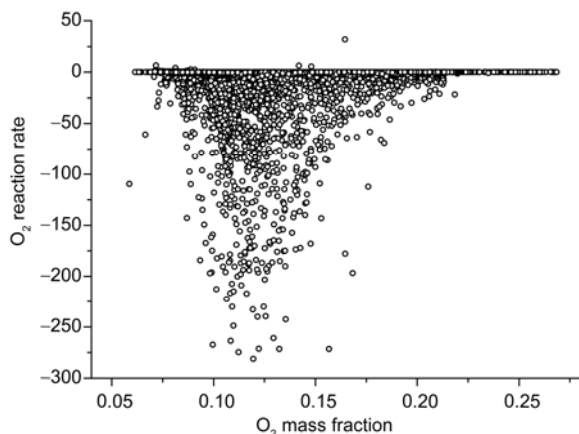
Table 1   Parameters of 1D PVDF used to generate training data

u' (m/s)	$Re_{u'}$	Range of k	k_e	Time scale (ms)
10	5600	0–2000	814.8	0.261
8	4480	0–1800	728.8	0.365
6	3360	0–1500	631.2	0.562
4	2240	0–1200	515.3	1.032
2	1120	0–900	364.4	2.920
1	560	0–600	257.7	8.260
0.5	280	0–500	182.2	23.361

C_3H_8/air case. In addition, total stepping time for each run was set to be 5 eddy turn-over time T_e. Required thermo-chemical states were recorded every $T_e/10$. A hyperplane of PVDF results for C_3H_8/air case, O_2 reaction rate along O_2 mass fraction (reaction progress), is shown in Figure 2. Turbulent effect on flame is well represented in the observed fluctuations.

1.2 ANN training

Back-propagation (BP) network [17] was adopted to memorize the collected sample states. For H_2/air case, QSS hypotheses is not imposed, so all involved species were designated to be inputs; for C_3H_8/air case, because 7 QSS species have been assumed, only remaining 20 species except N_2 are needed as inputs and their corresponding chemical rate as outputs. To improve model sensitivity to temperature, sample states were divided into 7 equi-distance bins along temperature value. Further, all data were standardized to range (0,1) before training. Tansig function was used as transfer function. Considering computational efficiency [12], two ANNs are both equipped with two hidden layers. After tentative calculations, ANN of H_2/air case uses 8 neurons for the first hidden layer and 4 for the second; ANN of C_3H_8/air cases is designed with 12 and 6 neurons accordingly. Scaled conjugate gradient (SCG) algorithm first

proposed by Møller [18] was employed for ANN training. Different from other conjugate gradient algorithm, this algorithm performs no line searches at each iteration. Thus, computation amount and the storage requirement, is largely reduced [19]. The training processes of 7 temperature-data bins for C_3H_8/air mixture are shown in Figure 3. To test ANN performance, 4000 thermo-chemical states are randomly selected from obtained database. Consequently ANN predicted reaction rates perfectly fit the authentic ones, as found in Figure 4. Up to now, ANN-based methods for both flames are constructed and can be directly integrated into following simulations to test the performance.

2 Numerical methodology for testing

2.1 DNS of flame-vortex interaction

Flame-vortex interaction (FVI) frequently occurs in turbulent combustion, and it represents the basic mode in which premixed flame is affected by vortex [4]. When a vortex penetrates through premixed flame, its leading edge first compresses the encountering flame and then entrainment
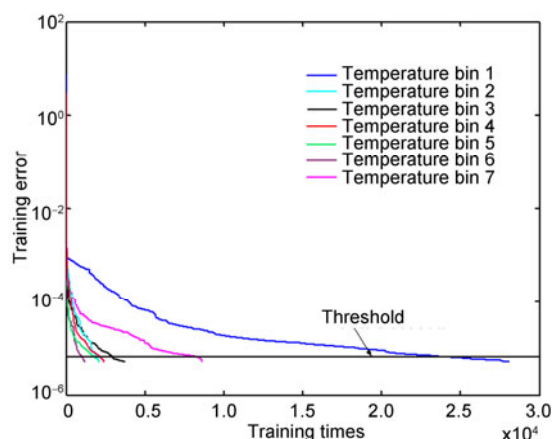
Figure 3   The training processes of all seven temperature-bins for C_3H_8/air mixture.

Figure 2   One hyperplane obtained using PVDF approach.
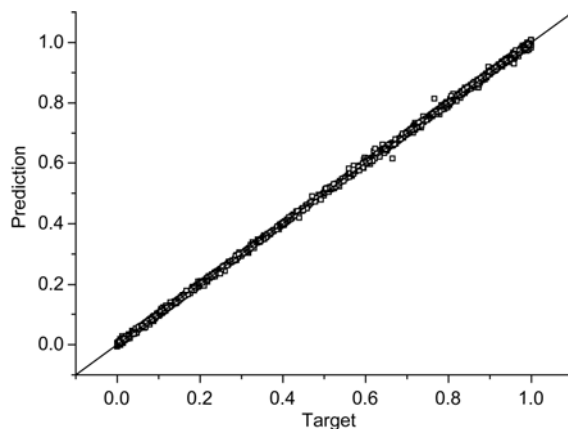
Figure 4   Performance of trained ANN.

effect causes the adjacent flame being gradually stretched. Consequently, as for the whole flame it experiences dynamically changing strain rate. Whether this process can be accurately modeled by the present method directly indicates its applicability to other models and processes. Thus, our method is designated to be firstly tested in FVI configuration by DNS.

The fully compressible Navier-Stokes equations were firstly nonnormalized, then differenced in eighth-order explicit scheme and then advanced temporarily using the fourth-order explicit Runge-Kutta method with CFL=0.06. Uniform meshes were used with spacing equal to two times of estimated Kolmogolov scale. A modified characteristics non-reflecting boundary condition, which encloses transverse source contribution [20], is imposed on all boundaries. All FVI test cases were initialized using individual laminar premixed flame and a pair of vortex. Laminar premixed flames for both H_2/air and C_3H_8/air cases were obtained by solving PREMIX [14]. The initial vortex pairs were always located in fresh mixture side at $10l_f$ away from the corresponding flame front. For a given moment, scalar profiles were drawn along the trace of one vortex center.

2.2 LES of turbulent Bunsen flame

LES of premixed flame has been applied in laboratorial scale [21] and even close to industrial application [22], with the rapid progress of computation ability. Moreover, to satisfy the requirement of modeling auto-ignition and slow-scale pollutants production in turbulent premixed flame, it has been believed that reduced mechanism with modest number of species will be initially used. Thus, it is necessary to test the applicability and performance of the present method in LES frame.

In LES, the closure of SGS stresses relies on Boussinesq hypothesis $\tau_{ij} - \tau_{kk}\delta_{ij}/3 = -2\mu_t \overline{S}_{ij}$, in which μ_t is the SGS turbulent viscosity, and $\overline{S}_{ij}$ is the rate-of-strain tensor for the resolved scale defined by $\overline{S}_{ij} = (\partial \overline{u}_i / \partial x_j + \partial \overline{u}_j / \partial x_i)/2$. μ_t is evaluated using the Dynamic Smagorinsky-

Lilly Model as proposed by Germano et al. [23] and Lilly [24], in which Smagorinsky constant is dynamically computed from local resolved motion to guarantee numerical stability [25]. Eddy-dissipation-concept (EDC) model [26] was adopted to account for combustion in subgrid. Detailed explanation can be found in [21]. For simplicity, LES was implemented in 2D based on finite-volume method. Pressure-velocity coupling was handled according to SIMPLE approach. Spatial differences are 3rd-order bounded center for momentum and second order upwind for others. The second-order accurate time derivative is

$$\frac{\partial \phi}{\partial t} = \frac{3\phi^{n+1} - 4\phi^n + \phi^{n-1}}{2\Delta t}. \tag{7}$$

Integration is implicit; convergence is achieved at each time step in ~20 iterations. Time step 6e-6s was set with CFL = 0.1. For all Bunsen flame cases, velocity, temperature and species concentrations are fixed at inflow boundary, while pressure outlet boundary condition is imposed on all outflow boundaries to ensure "well-posedness" [27]. The components of complementary flow are consistent with those of the corresponding burnt gas at individual adiabatic flame temperature.

3　Results and discussion

The performance test focuses on the accuracy, speed-up and storage of the proposed method. Each standard solution was obtained using the corresponding original detailed mechanisms and direct integration.

3.1　FVI test

Different vortex pairs were used in FVI test. H_2/air FVI cases were run with U_{max}/S_L equal to 26 and 39 while C_3H_8/air FVI cases were obtained at 33 and 66 U_{max}/S_L conditions. U_{max} is the maximum velocity induced by vortex. 2D contours with velocity vector plots, predicted using two methods, are shown in Figure 5. Furthermore, instantaneous profiles of scalars cross the individual flame are summarized in Figure 6.
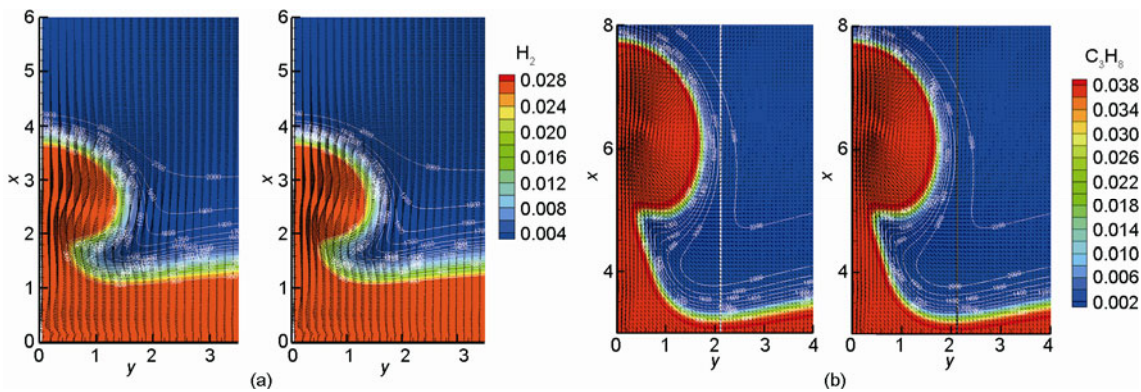

Figure 5　2D contours with velocity vectors predicted using DI and ANN for H_2/air FVI with $U_{max}/S_L = 26$ (a) and C_3H_8/air FVI with $U_{max}/S_L = 66$ (b): DI (left); ANN represented method (right). Colored by corresponding species mass fraction and lined by temperature value.
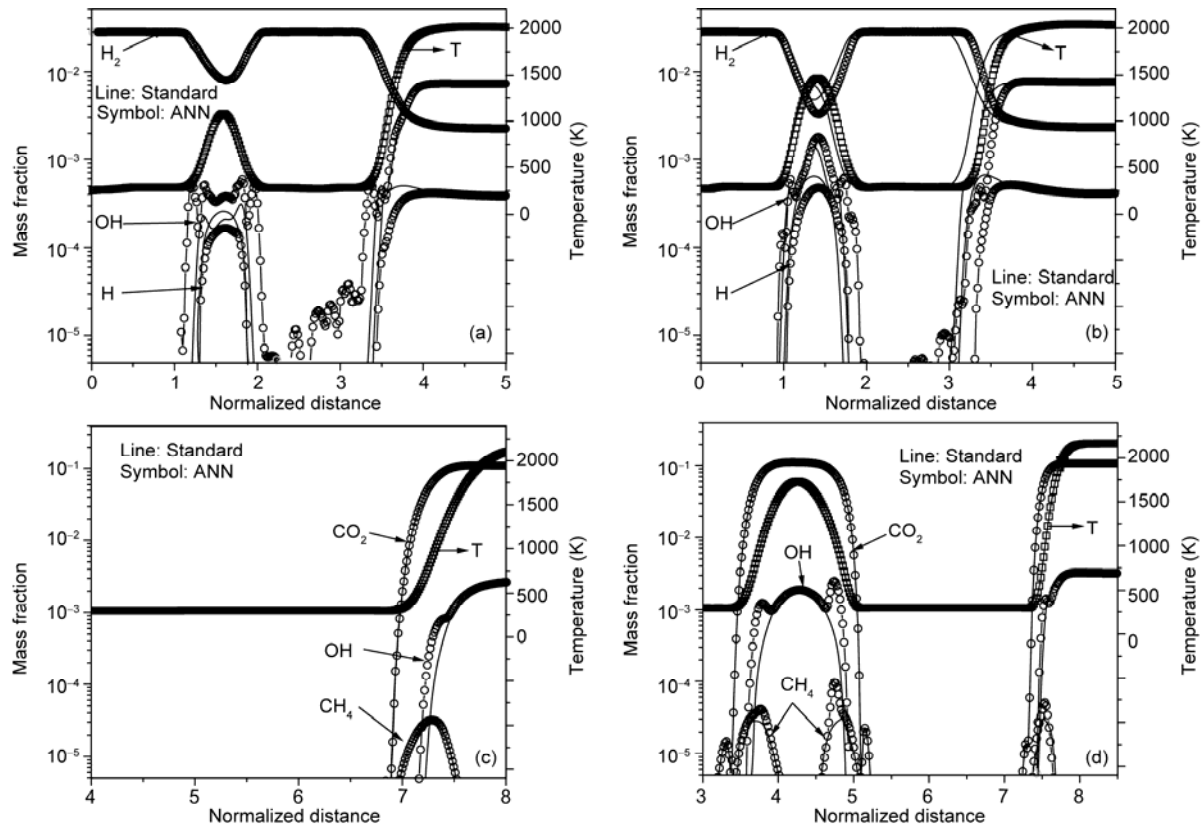
Figure 6 Instantaneous profiles of scalar variables in DNS of FVI. H_2/air case: (a) $U_{max}/S_L = 26$; (b) $U_{max}/S_L = 39$; C_3H_8/air case: (c) $U_{max}/S_L = 33$; (d) $U_{max}/S_L = 66$.

H_2/air FVI cases are shown in Figure 6(a) and (b) while C_3H_8/air FVI cases are in Figure 6(c) and (d). All predicted profiles well match with the corresponding standard ones. At all observed extremums, the relative errors of major species are not larger than 23%. On average errors are below 5% for major species and temperature. For minor species, such as OH, H and CH_4, errors are a little larger though profile agreements are still preserved. Predicted profiles of other involved species represent similar features even if not shown in figure. Comparatively scalar errors are a little larger in C_3H_8/air case than those in H_2/air case due to inclusion of kinetics reduction process, but by referring to the errors resulting from traditional reduced mechanism [9,28–31], the error magnitude is quite acceptable. Overall, the ANN-based method for chemical kinetics reduction can well replicate the flame dynamics in FVI at the influence of different vortex.

3.2 Bunsen-flame test

The instantaneous flame structures of the tested cases are shown in Figure 7. The H_2/air Bunsen flame uses fresh mixture inflow at 298 K with $1.5×10^5$ Reynolds number. The size of the jet is 70 mm, with the speed of 200 m/s centerflow and 1.8 m/s coflow. The inflow property of
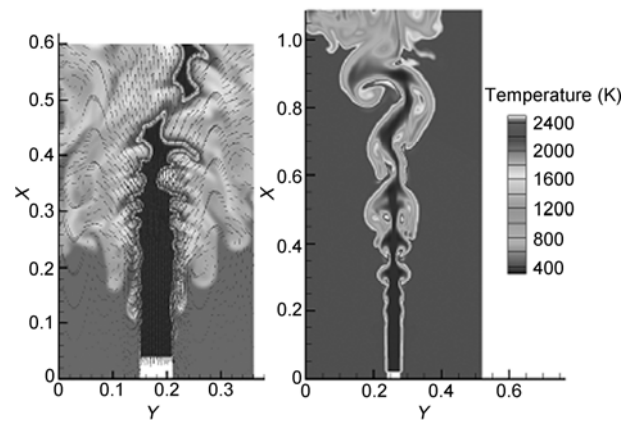

Figure 7 Instantaneous temperature fields of Bunsen-flame LES using ANN-based method for chemical kinetics reduction. (a) H_2/air case; (b) C_3H_8/air case.

C_3H_8/air flame is $6.2×10^4$ Reynolds number at 298 K. The size of the jet is 32 mm, with the speed of 8 m/s centerflow and 0.4 m/s coflow. Both grids are $L_x×L_y$ = 3 mm×3 mm, with stretch ratio of 1.05 in PML areas. As seen, along streamwise flame thickness is gradually increased and wrinkles become more obvious owing to vortex stretch effect. Comparatively C_3H_8/air flame is stretched to a more serious extent because of its much lower flame velocity.

Quantified accuracy evaluation is carried out by comparing ANN-based method predictions with the corresponding standard ones. Detailed comparisons of Favre-averaged scalar profiles have been exhibited in Figure 8. The predicted profiles are all in good agreement with standard solutions. Further, the relative errors of major species and temperature are around 13% and those of minor species are approximately 22%. Further, it is noticeable that the change of flame thicknesses and flame positions along streamwise is well resolved using the present method, especially in C_3H_8/air case. However, in some locations errors are larger for some minor species, such as C_2H_4 and O. The reason is probably the insensitivity of trained ANN to the used chemical sub-model in LES [32], which offers a good starting point for further improvement.

3.3 Speed-up and storage summary

For each case, the speed-up is defined as the ratio of running time using full mechanism with ANN-based method in each CFD time step. The running time used here actually include both time consumed for chemical reaction and fluid dynamics. As listed in Table 2, speed-ups obtained in DNS are relatively low. However, considering DNS usually run for many days or even several months, the absolute time actually saved is considerable. In LES, 13.6 speed-up obtained here is also larger than Sen and Menon's optimal value 11.2 in [12]. In addition, the required storage of our

method is very negligible, and thus it is still superior to other tabulation technics.

4 Conclusions

The construction and application of a novel ANN-based method for chemical kinetics reduction is discussed in detail. The PVDF approach is involved to quickly generate thermo-chemical states for ANN training. Pseudo-velocity, which can lead premixed flame to experiencing turbulence with various time and length scales, is introduced. The adaptability to different chemical kinetics, prediction accuracy, computational efficiency and storage of the method are highlighted in the performance test. H_2/air and C_3H_8/air turbulent premixed flames are modeled by DNS and LES integrated with this ANN-based method. The result shows that compared with ODE solutions using original detailed mechanism, the present method can well predict scalar profiles and error magnitudes of species concentrations and temperature are acceptable. Moreover, due to the involved

Table 2 Characteristic parameters of ANN-based method for both cases

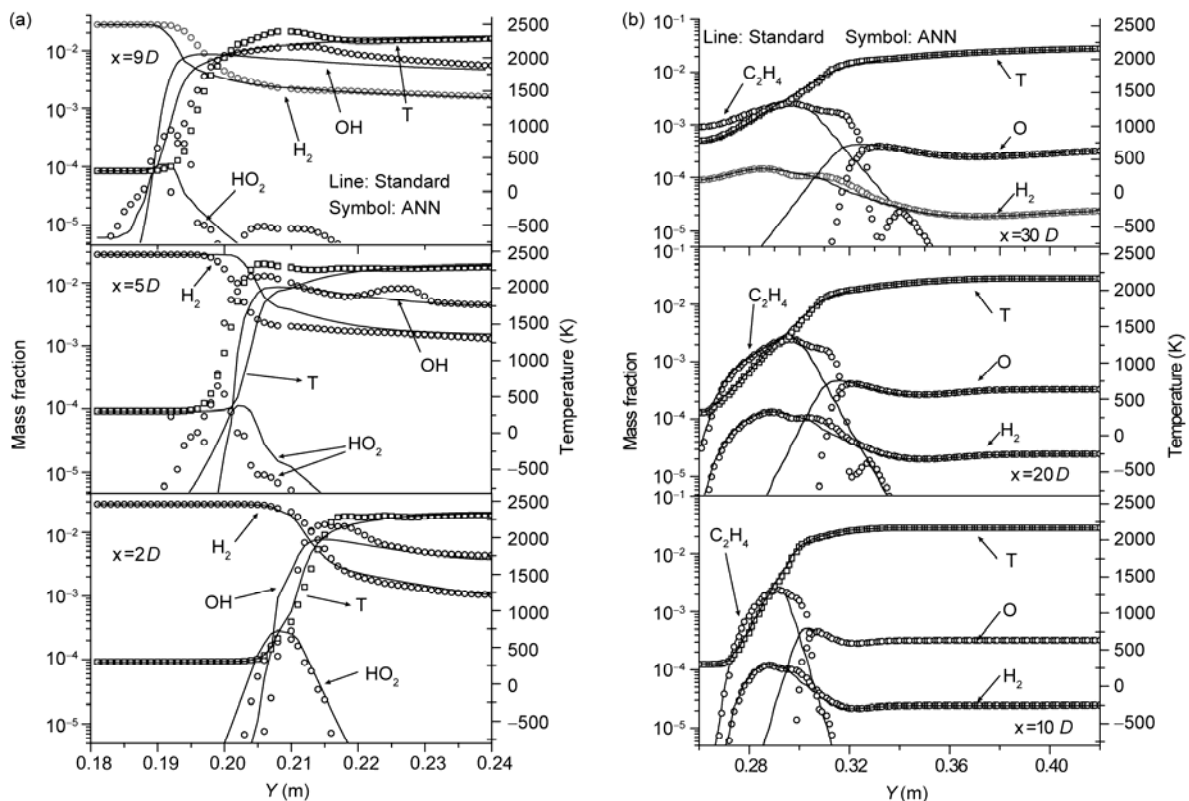| Case	Kinetics size	Table storage	ANN storage	Speed-up in DNS	Speed-up in LES
H_2/air	11 species	160 Mb	175 kb	1.05	8.2
C_3H_8/air	20 species	330 Mb	432 kb	1.42	13.6

Figure 8 Favre-averaged scalar profiles at different cross-sections downstream. (a) H_2/air case; (b) C_3H_8/air case.

mechanism reduction, C_3H_8/air case obtains a higher speed-up in LES than H_2/air case and previous study. The required storages of the present method for both cases are quite negligible (below 500 kb), much smaller than LUT and ISAT techniques. Thus, this method is more advantageous in memory-limited computations.

1   Venugopal R, Abraham J. A 2-D DNS investigation of extinction and reignition dynamics in nonpremixed flame-vortex interactions. Combust Flame, 2008, 153: 442–464

2   Lignell D O, Chen J H, Smith P J, et al. The effect of flame structure on soot formation and transport in turbulent nonpremixed flames using direct numerical simulation. Combust Flame, 2007, 151: 2–28

3   Xue H, Aggarwal S K. NO_x emissions in n-heptane/air partially premixed flames. Combust Flame, 2003, 132: 723–741

4   Kolera-Gokula H, Echekki T. Direct numerical simulation of premixed flame kernel-vortex interactions in hydrogen-air mixtures. Combust Flame, 2006, 146: 155–167

5   Tomlin A S, Turanyi T, Pilling M J. Comprehensive Chemical Kinetics. Amsterdam: Elsevier, 1997. 293–437

6   Lv Y, Wang Z, Zhou J, et al. Reduced mechanism for hybrid NO_x control process. Energy Fuels, 2009, 23: 5920–5928

7   Lu T, Law C K. A directed relation graph method for mechanism reduction. Proc Combust Inst, 2005, 30: 1333–1341

8   Lu T, Law C K. Linear time reduction of large kinetic mechanisms with directed relation graph: n-heptane and iso-octane. Combust Flame, 2006, 144: 24–36

9   Lv Y, Wang Z, Zhou J, et al. Development and validation of a reduced mechanism for urea-based SNCR process based on QSS graph. Energy Fuels, 2009, 23: 3605–3611

10 Chen J Y, Kollmann W, Dibble R W. Pdf modeling of turbulent nonpremixed methane jet flames. Combust Sci Tech, 1989, 64: 315–346

11 Pope S B. Computationally efficient implementation of combustion chemistry using in situ adaptive tabulation. Combust Theor Model, 1997, 1: 41–63

12 Sen B A, Menon S. Turbulent premixed flame modeling using artificial neural networks based chemical kinetics. Proc Combust Inst, 2009, 32: 1605–1611

13 Sen B A, Menon S. Artificial neural networks based chemistry-mixing subgrid model for LES. AIAA-07-0241, 47th Aerospace Science Meeting and Ex-hibit, 2007

14 Kee R J, Rupley F M, Miller J A. Chemkin-II: A fortran chemical kinetics package for the analysis of gas-phase chemical kinetics. Report No. SAND89-8009, Sandia National Laboratories, 1989

15 Haworth D C, Blint R J, Cuenot B, et al. Numerical simulation of turbulent propane-air combustion with nonhomogeneous reactants. Combust Flame, 2000, 121: 395–417

16 Passot T, Pouquet A. Numerical simulation of compressible homogeneous flows in the turbulent regime. J Fluid Mech, 1987, 181: 441–466

17 Rumelhart D E, Hinton G E, Williams R J. Learning representations by back-propagating errors. Nature, 1986, 323: 533–536

18 Møller M F. A scaled conjugate gradient algorithm for fast supervised learning. Neural Networks, 1993, 6: 525–533

19 Plumb A P, Rowe R C, York P, et al. Optimisation of the predictive ability of artificial neural network (ANN) models: A comparison of three ANN programs and four classes of training algorithm. Europ J Pharm Sci, 2005, 25: 395–405

20 Lodato G, Domingo P, Vervisch L. Three-dimensional boundary conditions for direct and large-eddy simulation of compressible viscous flows. J Comput Phys, 2008, 227: 5105–5143

21 Giacomazzi E, Battaglia V, Bruno C. The coupling of turbulence and chemistry in a premixed bluff-body flame as studied by LES. Combust Flame, 2004, 138: 320–335

22 Boileau M, Staffelbach G, Cuenot B, et al. LES of an ignition sequence in a gas turbine engine. Combust Flame, 2008, 154: 2–22

23 Germano M, Piomelli U, Moin P, et al. A dynamic subgrid-scale eddy viscosity model. Phys Fluids A: Fluid Dyn, 1991, 3: 1760–1765

24 Lilly D K. A proposed modification of the Germano subgrid-scale closure method. Phys Fluids A: Fluid Dyn, 1992, 4: 633–635

25 Kim S E. Large eddy simulation using unstructured meshes and dynamic subgrid-scale turbulence models. AIAA-2004-2548, 34th Fluid Dynamics Conference and Exhibit, 2004

26 Magnussen B F, Hjertager B H. On mathematical modeling of turbulent combustion with special emphasis on soot formation and combustion. Int Symp Combust, 1977, 16: 719–729

27 Poinsot T J, Lelef S K. Boundary conditions for direct simulations of compressible viscous flows. J Comput Phys, 1992, 101: 104–129

28 Giral I, Alzueta M U. An augmented reduced mechanism for the reburning process. Fuel, 2002, 81: 2263–2275

29 Mendiara T, Alzueta M U, Millera A, et al. An augmented reduced mechanism for methane combustion. Energy Fuels, 2004, 18: 619–627

30 Xu H, Smoot L D, Hill S C. A reduced kinetic model for NO_x reduction by advanced reburning. Energy Fuels, 1998, 12: 1278–1289

31 Xu H, Smoot L D, Hill S C. Computational model for NO_x reduction by advanced reburning. Energy Fuels, 1999, 13: 411–420

32 Sen B A, Menon S. Linear eddy mixing based tabulation and artificial neural networks for large eddy sim-ulations of turbulent flames. Combust Flame, 2010, 157: 62–74